ARTICLE OPEN

Check for updates

Nanomechanical cat states generated by a dc voltage-driven Cooper pair box qubit

Danko Radić[1], Sang-Jun Choi[2,3], Hee Chul Park[2]✉, Junho Suh[4], Robert I. Shekhter[5] and Leonid Y. Gorelik[6]

We study a nanoelectromechanical system consisting of a Cooper pair box qubit performing nanomechanical vibrations between two bulk superconductors. We demonstrate that a bias voltage applied to the superconductors may generate states represented by entanglement between qubit states and quantum 'cat states', i.e. a superposition of the coherent states of the nanomechanical oscillator. We characterize the formation and development of such states in terms of the corresponding Wigner function and entropy of entanglement. Also, we propose an experimentally feasible detection scheme for the effect, in which the average current that attains the specific features created by the entanglement is measured.

npj Quantum Information (2022)8:74 ; https://doi.org/10.1038/s41534-022-00584-6

INTRODUCTION

Electro-mechanical and mechano-electrical transduction phenomena acquire whole new dimensions on the mesoscopic scale. A number of novel functionalities have resulted from new physics that gains relevance on nanometer length scales where quantum mechanics and Coulomb correlations play a crucial role. Phonon-assisted tunneling[1–6], the rectification of ac current[7–9], and the mechanical transportation of single electrons[10] are just a few examples of mechanically assisted electronics. Nanoelectromechanical (NEM) devices further allow for control over the mechanical subsystem by electron transportation. Ground state cooling[11,12] and shuttle instability[4,13] present good illustrations of such control.

Superconducting ordering brings new qualitative features to the functioning of NEM devices. It has been shown that the mechanical transportation of Cooper pairs can facilitate a superconducting current and generate Josephson coupling between remote superconductors[14–16]. A natural question, then, arises: how will the coherent dynamics of a superconducting circuit affect the nanomechanical performance of a NEM system? The coherent interplay between the states of superconducting qubits and mechanical excitations is a focus of modern frontline research in quantum communication[17–22]. Recently, it was demonstrated that individual phonons can be controlled and detected by a superconductor qubit, enabling the coherent generation and measurement of a non-classical superposition of the zero- and one-phonon Fock states[21,22]. This control allows one to accomplish phonon-mediated quantum state transfer and establish remote qubit entanglement. On the other hand, a mechanical resonator provides the possibility to store quantum information in complex multi-phonon states, so-called (Schrödinger) 'cat states'. Such states, rather resilient to external perturbation, allow quantum information to be encoded in such a way that mechanical losses can be detected and corrected, as opposed to single-phonon states where such losses irreversibly delete the quantum information[23]. The realization of cat-states is also vastly utilized in optics[24]. In this letter, we consider the possibility to generate quantum entanglement between a charge qubit and a nanomechanical resonator, and to encode the qubit states in the nanomechanical cat states.

RESULTS

Schematic diagram of experimental setup

A schematic of the nanomechanical charge qubit under consideration is presented in Fig. 1. The system consists of a superconducting island, positioned between two bulk superconductors, able to perform mechanical motion between them. We suppose that the island is attached to, for example, the top of a cantilever whose mechanical motion is described by a harmonic oscillator. The gate electrode induces an electrical potential on the island. In this work, we treat the superconducting island as a charge qubit, i.e., a Cooper pair box (CPB) whose basis states are charge states, for example, states that represent the presence or absence of one excess Cooper pair on the island; we refer to these states as charged and neutral states. Tunnel coupling between the CPB and the bulk superconducting electrodes induces transitions between the qubit states, with a transition amplitude that depends on the distance between the island and electrodes as well as on the value of the superconducting phase. Bias voltage V, applied between the bulk superconducting electrodes, generates a time evolution of the superconducting phase difference Φ according to the Josephson relation $\dot{\Phi}(t) = 2eV(t)/\hbar$.

Time evolution of entangled ground state

Hamiltonian $\widehat{H}$, describing the joined dynamics of the charge qubit and the cantilever (for details see Supplemental material, Section II), can be presented as $\widehat{H} = \widehat{H}_0 + \widehat{H}_1$, where

$$\widehat{H}_0 = E_J \cos(\Phi(t))\hat{\sigma}_1 + \hbar\omega\left(\frac{\widehat{p}^2}{2} + \frac{\widehat{x}^2}{2}\right)$$
$$\widehat{H}_1 = \varepsilon E_J \hat{x} \sin(\Phi(t))\hat{\sigma}_2. \quad (1)$$

The first term in $\widehat{H}_0$ describes the position-independent part of the tunnel coupling between the CPB and bulk superconductors,

[1]Department of Physics, Faculty of Science, University of Zagreb, Bijenička 32, Zagreb 10000, Croatia. [2]Center for Theoretical Physics of Complex Systems, Institute for Basic Science (IBS), Daejeon 34051, Republic of Korea. [3]Institute for Theoretical Physics and Astrophysics, University of Würzburg, D-97074 Würzburg, Germany. [4]Korea Research Institute of Standards and Science, Daejeon, Republic of Korea. [5]Department of Physics, University of Gothenburg, SE-412 96 Göteborg, Sweden. [6]Chalmers University of Technology, SE-412 96 Göteborg, Sweden. ✉email: hcpark@ibs.re.kr

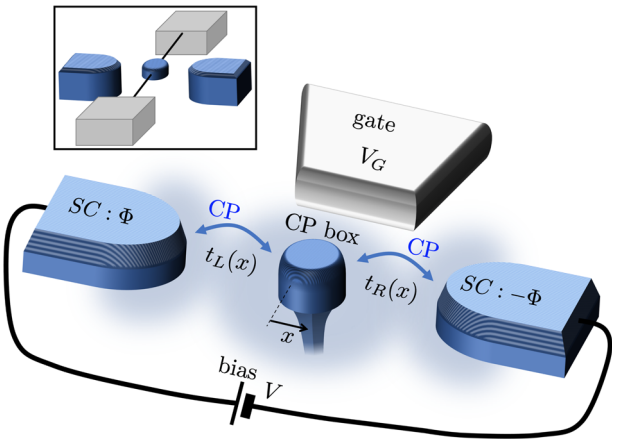

Fig. 1 Schematic presentation of the proposed junction. There are two bulk superconducting contacts with phases $\pm\Phi$ biased by voltage V with a superconducting island (Cooper pair box—CPB) in between. $t_{L(R)}(x)$ are the tunneling amplitudes for the Cooper pairs between the leads and the CP box, dependent on position x. V_G is the gate voltage. Two possible configurations are presented: the CPB island on the top of the oscillating cantilever (main figure), and the CPB island attached in the middle of the suspended oscillating nanowire with V_G provided via the substrate (inset). For equivalent electrical circuit see Supplemental material, Section I, Fig. 1.

where E_J is the Josephson energy. Here, $\hat{\sigma}_i$, $i=1,2,3$ are the Pauli matrices acting in charge qubit Hilbert space, particularly in the basis where vectors $(1,0)$ and $(0,1)$ represent charged and neutral states, respectively. The second term in $\widehat{H}_0$ describes the mechanical subsystem with momentum $\widehat{p}$ and coordinate $\widehat{x}$ of the mechanical oscillator normalized to the amplitude of the zero mode vibrations $x_0=\sqrt{\hbar/m\omega}$, where m is the mass of the oscillator and $\omega=2\pi/T$ is its frequency. Hamiltonian $\widehat{H}_1$ describes the coupling between the nanomechanical and electronic subsystems, induced by the position-dependant part of the tunnel coupling. Here, $\varepsilon\equiv x_0/x_{tun}\ll 1$ is a small coupling parameter (x_{tun} is the tunneling length). We consider the regime in which $\Phi=0$ for $t<0$ and $V(t)=V\Theta(t)$, where $\Theta(t)$ is the Heaviside step function. For $t<0$, the interaction between the subsystems is switched off and the system is in the *pure* state $\boldsymbol{e}_{in}\otimes|0\rangle$. Here, $|0\rangle$ is the ground state of the mechanical oscillator, and $\boldsymbol{e}_{in}=\sum_\kappa c_i^\kappa \boldsymbol{e}_\kappa^i$ is the initial state of the CPB where $\boldsymbol{e}_\kappa^i$ are eigenvectors of Pauli matrices $\hat{\sigma}_i$ with eigenvalues $\kappa=\pm1$. For $t>0$, a constant bias voltage is switched on and the Josephson phase linearly increases in time, i.e., $\Phi(t)=\Omega_V t$, where $\Omega_V\equiv 2\pi/T_V=2|eV|/\hbar$. To describe the time evolution of the system at $t>0$, one can use the interaction representation for the time evolution operator in the form

$$\widehat{U}(t,t')=\widehat{U}_0(t)\widehat{U}_1(t,t')\widehat{U}_0^\dagger(t'). \tag{2}$$

Here, $\widehat{U}_0(t)=\exp\left(-\frac{i}{\hbar}\int_0^t\widehat{H}_0(\tilde{t})d\tilde{t}\right)$ and $\widehat{U}_1(t,t')$ is given by the equation

$$i\hbar\frac{d\widehat{U}_1(t,t')}{dt}=\varepsilon E_J\hat{x}(t)\sin(\Phi(t))\hat{\sigma}_2(t)\widehat{U}_1(t,t'),\ \widehat{U}_1(t,t)=1, \tag{3}$$

where $\hat{x}(t)=\hat{x}(t+T)$ and $\hat{\sigma}_2(t)=\hat{\sigma}_2(t+T_V)$ are operators in the interaction picture. If the frequencies ω and Ω_V are incommensurable, then the product $\hat{x}(t)\hat{\sigma}_2(t)$ oscillates quasi-periodically in time, and as a consequence, the mechanical subsystem remains in the vicinity of the ground state if $\varepsilon E_J\ll\hbar\omega$. However, in the 'resonant' case when $\omega=l\Omega_V$ and l is positive integer, the number of phonons increases in time and entanglement arises between the qubit states and the macroscopically excited states of the nanomechanical resonator. We perform analysis within the framework of rotating wave approximation, namely, we change the periodic functions of time, appearing in Eq. (3), with their average values over one period. The evolution operator is obtained in the form

$$\widehat{U}_1(t,t')=\begin{cases}e^{\frac{i}{2\hbar}\varepsilon E_J A_l\hat{\sigma}_2\widehat{p}(t-t')}, & l=1,3,5\ldots\\ e^{\frac{i}{2\hbar}\varepsilon E_J A_l\hat{\sigma}_3\widehat{x}(t-t')}, & l=2,4,6\ldots\end{cases} \tag{4}$$

where $A_l=(-1)^l\mathrm{sgn}(eV)\left(\mathrm{J}_{l-1}\left(\frac{2E_J}{\hbar\Omega_V}\right)-\mathrm{J}_{l+1}\left(\frac{2E_J}{\hbar\Omega_V}\right)\right)$, and $\mathrm{J}_l(x)$ are the Bessel functions of the first kind. In this paper, we only consider the case $l=1$, i.e. $\omega=\Omega_V$.

Nanomechanical cat states

Applying the operators from Eqs. (2) and (4) to the initial state, we obtain the state of the system at time t:

$$|\boldsymbol{\Psi}(t)\rangle=\sum_\kappa c_2^\kappa\boldsymbol{e}_\kappa^2(t)\otimes|a_\kappa(t,0)\rangle. \tag{5}$$

In this equation, $\boldsymbol{e}_\kappa^2(t)=\exp\left(-i\frac{E_J}{\hbar\omega}\sin(\omega t)\hat{\sigma}_1\right)\boldsymbol{e}_\kappa^2$, and $|a_\kappa(t,\xi)\rangle$ denotes the coherent states such as $\hat{a}|a_\kappa(t,\xi)\rangle=\kappa v(t-\xi)\exp(i\omega t)|a_\kappa(t,\xi)\rangle$ with $v=\varepsilon A_1E_J/\hbar$, where $\hat{a}$ is the phonon annihilation operator. We should note that the rotating wave approximation is valid only if the energy of interaction between the qubit and the resonator, being of the order of $\varepsilon A_1E_J\sqrt{\langle\hat{x}^2\rangle}$, is smaller than $\hbar\omega$. This sets a restriction on time t, for which Eq. (5) is valid, to $t\le(\varepsilon v)^{-1}$. Time t should also be shorter than any relaxation and dephasing time t_0, which is discussed in the last section. There we give an estimation of the experimental feasibility of the proposed effect for typical values of parameters.

In the resonant case, numerical computation of the time evolution of the ground state shows entanglement of the CPB charged states with the mechanical coherent states whose amplitude linearly increases in time. On the other hand, the off-resonant case ($\omega\neq l\Omega_V$) exhibits an evolution of the ground state that does not form coherent states, providing that the amplitude does not increase monotonically over time. In numerics, we prepare the Hilbert space in the basis of Fock states $\mathbf{e}_\kappa^2\bigotimes|n\rangle$ where $\hat{a}^\dagger\hat{a}|n\rangle=n|n\rangle$. The initial ground state is taken as $\mathbf{e}_{-1}^1\bigotimes|0\rangle$. To analyze the numerical results, we use the functional form for an arbitrary quantum state as $|\Psi(t)\rangle=\sum_{n=0}^{n_{max}}(C_n\mathbf{e}_{+1}^2\bigotimes|n\rangle-D_n\mathbf{e}_{-1}^2\bigotimes|n\rangle)$, and we find that $D_n=(-1)^nC_n$ due to the symmetry $[\widehat{H},\widehat{P}]=0$, where $\widehat{P}=(-1)^{\hat{n}}\hat{\sigma}_1$. To compare the resonant and off-resonant cases, we plot two numerical results obtained for $\omega=\Omega_V$ and $\omega=1.01\Omega_V$ in Fig. 2. Numerical analysis of the distribution of $|C_n|$, using $D_n=(-1)^nC_n$, shows that the time-evolved state in the resonant case is an entangled quantum state between the coherent states of the mechanical resonator and the states of the CPB qubit.

Since $v=0$ when $V=0$, one can control the entanglement described above by switching the bias voltage on and off. Let us consider the following time protocol: we switch off the voltage at time $t_s=N_sT$, where N_s is integer, and we keep $V=0$ during one period T, after which we switch on the voltage again (a general case for the arbitrary switch-on and switch-off times is presented in Supplemental material, Section III). During that single period, the time evolution is governed by operator $\tilde{U}(t)=\exp[\frac{i}{\hbar}(t-t_s)(E_J\sigma_1+\hbar\omega\hat{a}^\dagger\hat{a})]$. Using Eqs. (2), (4), and (5), for $t>t_s+T$, we find that the state of the system is given by the expression

$$|\boldsymbol{\Psi}(t)\rangle=\sum_\kappa c_2^\kappa\boldsymbol{e}_\kappa^2(t)\otimes\{\rho|a_\kappa(t-T,0)\rangle+i\tau|a_{-\kappa}(t-T,2(t_s-T))\rangle\};\quad\rho=\cos\left(\tfrac{2\pi E_J}{\hbar\omega}\right),\ \tau=\sin\left(\tfrac{2\pi E_J}{\hbar\omega}\right);\ \rho^2+\tau^2=1. \tag{6}$$

One can see that for $t>t_s+T$ the state of the system is represented by the entanglement of the qubit states with two cat states of the mechanical resonator.

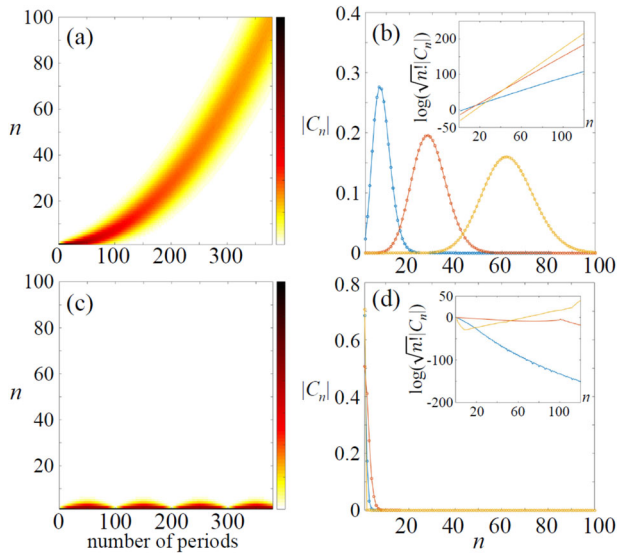

Fig. 2 Time evolution of the ground state. For $\omega = \Omega_V$ ($\omega = 1.01\Omega_V$), the time evolution is plotted in the top (bottom) panels. The intensity of $|C_n|$ is presented via colormap as a function of t and n in a, c. To exhibit the evolution of the coherent states, $|C_n|$ is displayed at specific moments $t = 100T, 200T, 300T$ in (**b**) and $t = 10T, 50T, 100T$ in (**d**). Insets show that $\log(\sqrt{n!}|C_n|)$ is linearly increasing as a function of n in the resonant case $\omega = \Omega_V$, which is equivalently $|C_n| \propto |\alpha|^n/\sqrt{n!}$. The slope of $\log(\sqrt{n!}|C_n|)$ determines α. We use the following parameters: $E_J = 1$, $\omega = 1/1.4$, $\epsilon = 0.01$, $n_{max} = 120$; $\hbar \equiv 1$.

Entropy of entanglement

To characterize the entanglement between the qubit and the mechanical subsystem, we use the reduced density matrix $\widehat{\varrho}_{q(m)}(t) = \mathrm{Tr}_{m(q)}\widehat{\varrho}(t)$, where $\widehat{\varrho}(t) = |\boldsymbol{\Psi}(t)\rangle\langle\boldsymbol{\Psi}(t)|$. $\widehat{\varrho}_{q(m)}$ are reduced density matrices with respect to tracing out mechanical or qubit degrees of freedom, respectively. In particular, using Eq. (6) we find that when $\boldsymbol{e}_{in} = \boldsymbol{e}^1_{-1}$, the reduced density matrix $\widehat{\varrho}_q(t)$ takes the form

$$\begin{aligned} &\widehat{\varrho}_q(t) = \tfrac{1}{2} - \tfrac{1}{2}\lambda(t,t_s)\hat{\sigma}_1; \\ &\lambda(t,t_s) = e^{-2v^2t^2}, \quad 0 < t \le t_s \\ &\lambda(t,t_s) = \rho^2 e^{-2v^2(t-T)^2} + \tau^2 e^{-2v^2(t-2t_s+T)^2}, \quad t > t_s + T. \end{aligned} \tag{7}$$

This expression allows us to calculate the entropy of entanglement, $S_{en}(t) \equiv \mathrm{Tr}\,\widehat{\rho}_q(t)\log\widehat{\rho}_q(t) = \mathrm{Tr}\,\widehat{\rho}_m(t)\log\widehat{\rho}_m(t)$. A plot of $S_{en}(t)$ for $vt_s = 0.5$ and different values of ρ is presented in Fig. 3. One can find that $S_{en}(t)$ monotonically increases in time before the bias voltage is switched off at $t = t_s$. For $t_s < t < t_s + T$, $S_{en} = const$ due to the switched-off interaction between the CPB and mechanical subsystem. For $t > t_s + T$, the entanglement entropy depends on ρ, as follows: for $\rho > 1/\sqrt{2}$, $S_{en}(t)$ continues to grow monotonically, while for $\rho < 1/\sqrt{2}$, $S_{en}(t)$ starts to decrease, reaches some minimal value (which equals zero for $\rho = 0$), and then grows again. However, regardless of the value of ρ, $S_{en}(t)$ saturates to a maximal value of $\log 2$ for $t \to \infty$.

The Wigner function of cat states

To characterize the state of the mechanical subsystem, it is convenient to use the Wigner function $W(x,p,t) = (\hbar\pi)^{-1}\int \varrho(x+y, x-y, t)\,\exp(i2py/\hbar)dy$, where $\varrho(x_1, x_2, t)$ is the density matrix in $x-$ representation. A plot of $W(x,p,t)$ is presented in Fig. 4 for $\rho = 1/\sqrt{2}$ at two different times, $t = t_s$ in (a) and $t = 3t_s$ in (b).

From Fig. 4, one can see that at $t = t_s$, the Wigner function is positive and has two peaks, demonstrating entanglement between two-qubit states and two coherent states. This feature exists for all times $t < t_s$. After switching off the bias voltage at $t = t_s$ and then switching it back on at $t = t_s + T$, the Wigner function takes both positive and negative values, demonstrating entanglement between two-qubit states and two cat states of the mechanical subsystem.

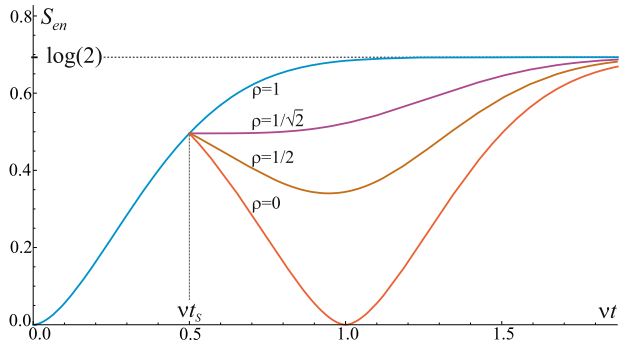

Fig. 3 Entropy of entanglement. Entropy S_{en} is plotted dependent on time t for different values of ρ with $E_J/\hbar\omega = 1.4$. For $t_s < t < t_s + T$, $S_{en} = const$ (not shown in the figure).

Electric current through the junction

Following the discussion above, the amplitude of the mechanical vibration increases in time, and the energy stored in the mechanical subsystem also increases. This energy supply comes from the electronic subsystem and may give rise to a rectification of the ac Josephson current induced by the bias voltage. To investigate this phenomenon, we calculate current $I(t)$, produced by the bias voltage, and take its average over the period T, i.e. $\langle I(N)\rangle_T = T^{-1}\int_{NT}^{(N+1)T} I(t)\mathrm{d}t$, $N = 0, 1, 2, \ldots$ The power, $P = V \cdot I$, absorbed by the system is determined by the change of mechanical energy ΔE_m and qubit energy ΔE_q after the $(N+1)$-th period. Using the reduced density matrix for mechanical $\widehat{\varrho}_m$ and qubit $\widehat{\varrho}_q$ subsystems, we calculate $\langle I(N)\rangle_T$ for $\boldsymbol{e}_{in} = \boldsymbol{e}^1_{-1}$ and different values of ρ with

$$\langle I(N)\rangle_T = \frac{e\omega}{2\pi}\nabla_N\left((vNT)^2 - \frac{E_J}{\hbar\omega}\lambda(vNT, t_s)\right), \tag{8}$$

where $\nabla_N f(N) \equiv f(N) - f(N-1)$ is the first difference, and the first and second contributions in Eq. (8) are ΔE_m and ΔE_q, respectively. Results for different values of ρ with $vt_s = 3$ and $E_J/\hbar\omega = 1.4$ are presented in Fig. 5.

From Eq. (7), one can see that for $vt \gg vt_s \gg 1$, the eigenvalue λ decays exponentially, and therefore the main contribution to the current comes from the mechanical subsystem, and it linearly increases in time (see Fig. 5). The non-monotonic feature of t of the order of t_s comes from the non-monotonic absorption of power by the qubit subsystem. It is pronounced around $t = 0$ (before t_s) when the evolution of the system from the ground state begins. During the period with switched-off voltage, the current is zero, i.e., $\langle I(N_s)\rangle_T = 0$. At the moment $t = t_s + T$, the current exhibits a jump originating from the fact that it changes depending on amplitudes ρ and τ. For $\rho = 1$, the current continues to flow in the same direction, while for $\rho = 0$ it changes direction completely thus switching its sign. For $\rho = \tau = 1/\sqrt{2}$, two contributions of the current flowing in opposite directions exactly cancel each other, giving zero current at $t = t_s + T$.

Experimental feasibility

To give an estimation of the experimental feasibility of the proposed effect, we take typical values of the charge CPB qubit: decoherence time $t_0 \approx 1\,\mu$s (for different possible mechanisms leading to decoherence see Supplemental material, Section IV: A —phonon loss of the mechanical oscillator, B—charge flip of the

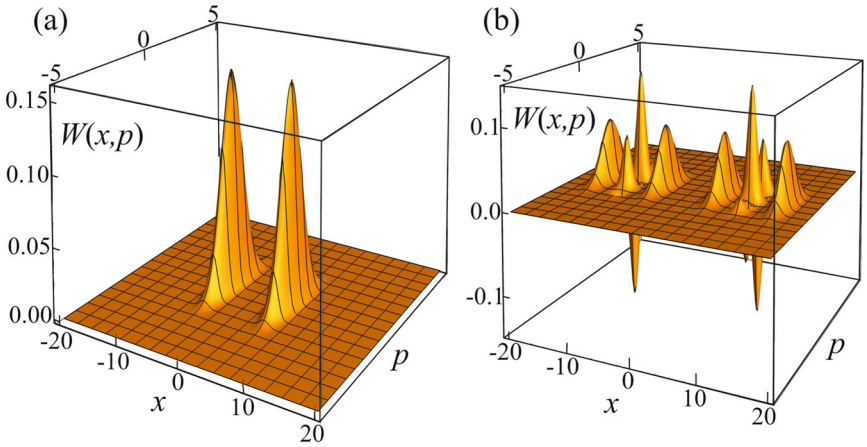

Fig. 4 Wigner function of cat states. The Wigner function $W(x, p)$ for $\rho = \tau = 1/\sqrt{2}$ and $E_J/\hbar\omega = 1.4$ is plotted at time (**a**) $t = t_s$ and (**b**) $t = 3t_s$, for $vt_s = 5$. Two entangled states of qubit and nanomechanical oscillator develop in time (**a**) and, after applying the protocol with bias voltage, two cat states emerge (**b**).

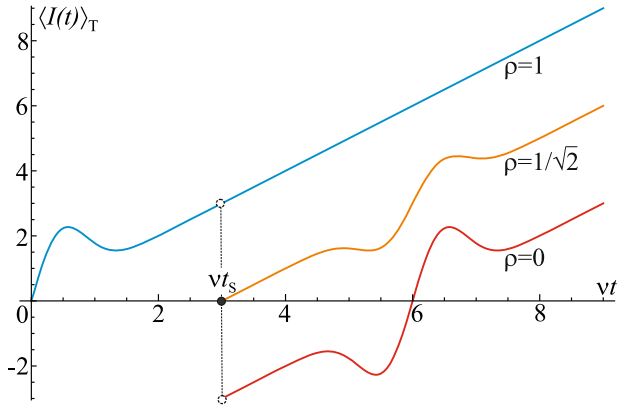

Fig. 5 Average current (over period *T*). Average current $\langle I(t)\rangle_T$ is plotted dependent on time t for mechanical frequency of 1GHz, ratio $E_J/\hbar\omega = 1.4$ and different values of ρ (continuous lines are interpolated through the $\langle I(N)\rangle_T$ points, $\langle I(N_s)\rangle_T \to \langle I(t_s)\rangle_T = 0$).

CPB, C— both mechanisms, as well as refs. [25,26]), Josephson energy $E_J \approx 0.1 \div 1K$, tunneling length $x_{tun} \approx 1$Å, and mass of the oscillator $m \approx 10^{-22} \div 10^{-21}$kg[27], providing the coupling strength $\varepsilon E_J \sim 0.01 \div 0.1$K. Then, using an asymptotic form of the Bessel function in A_l coefficient in Eq. (4), we estimate a shift of the mechanical coherent state with respect to the origin for a given time t_0, $X \approx \sqrt{\frac{E_J}{\pi m}}\frac{x_0}{x_{tun}} t_0 \sim 10^2 \div 10^3 x_0$. Furthermore, using numerical simulations we show that coherent dynamics is preserved even above validity interval of the rotating wave approximation that we used to obtain the analytical results (see Fig. 2 and Supplemental material, Section IV, Figs. 2–7), i.e., during ~10^3 periods of mechanical vibrations. For mechanical oscillator at 10 GHz (such frequency corresponds e.g. to the 3rd bending mode of the suspended CNT or some other setup[27–30]) and a corresponding bias voltage of the order of 10 μV, which can be controlled fairly well to preserve the resonance to accuracy 0.1% (commercially available voltage sources, e.g., Keysight B2961A manufactured by Keysight Technologies) we obtain current, containing the predicted feature, of the order of nanoamp. Our preliminary analysis has revealed that effects qualitatively similar to those presented in this letter likewise take place in the transmon design of charge qubits (when the Josephson energy is larger than the charging energy) if the mechanical frequency is much smaller compared to the charging energy, and if the degeneracy of the qubit energy level at a certain phase difference is preserved.

DISCUSSION

We have analyzed the quantum dynamics of a NEM system comprising a movable CPB qubit that mechanically (harmonically) oscillates between two bulk superconductors coupled to the CPB via Cooper pair tunneling controlled by bias voltage. We demonstrate, analytically and numerically, that when the ac Josephson frequency of the superconductors is in resonance with the mechanical frequency of the CPB, the initial pure state (direct product of the CPB ground state and the oscillator state with zero phonons) evolves in time as the coherent states of the mechanical oscillator entangled with the qubit states. Furthermore, we establish a protocol for bias voltage manipulation that results in the formation of entangled states incorporating so-called cat states, i.e., a quantum superposition of the nanomechanical coherent states. The formation of such states is confirmed by analysis of the corresponding (negative) Wigner function, while their specific features provide for the possibility of experimental detection by measuring the average current. The discussed phenomena may serve as a foundation for the encoding of quantum information from charge qubits into (superpositions of) coherent mechanical states. As such, this work may constitute an important tool in the field of quantum communications due to the robustness of the multi-phonon states with respect to external perturbation, compared to the single-phonon Fock state. Discussion of the specific protocols for such encoding, though, are out of the scope of this work and will be presented elsewhere. In contrast to suggestions for mechanical cat states[31–34] generated either “electrically" (via strong polaronic effect), or “optically" (driving the mechanics by electromagnetic field), the phenomenon discussed in this paper allows entangling the NEM cat states with a superconducting charge qubit, providing the transfer of quantum information between the superconducting qubit to mechanical vibrations. Potentially, this may lead to a chance of exploring the possibility of achieving quantum communication utilizing the semiclassical mechanical (vibrational) cat states.

DATA AVAILABILITY

The data that support the findings of this study are available from the corresponding author upon reasonable request.

Received: 22 October 2021; Accepted: 17 May 2022;
Published online: 27 June 2022

REFERENCES

1. Jaklevic, R. C. & Lambe, J. Molecular vibration spectra by electron tunneling. *Phys. Rev. Lett.* **17**, 1139–1140 (1966).
2. Glazman, L. I. & Shekhter, R. I. Inelastic resonant tunneling of electrons through a potential barrier. *Zh. Eksp. Teor. Fiz* **94**, 292 (1988); *Sov. Phys. JETP* **67**, 163–170 (1988).
3. Stipe, B. C., Rezaei, M. A. & Ho, W. Single-molecule vibrational spectroscopy and microscopy. *Science* **280**, 1732–1735 (1998).
4. Park, H. et al. Nanomechanical oscillations in a single-C60 transistor. *Nature* **407**, 57–60 (2000).
5. Park, J. et al. Coulomb blockade and the Kondo effect in single-atom transistors. *Nature* **417**, 722–725 (2002).
6. Smit, R. H. M. et al. Measurement of the conductance of a hydrogen molecule. *Nature* **419**, 906–909 (2002).
7. Ahn, K.-H., Park, H. C., Wiersig, J. & Hong, J. Current rectification by spontaneous symmetry breaking in coupled nanomechanical shuttles. *Phys. Rev. Lett.* **97**, 216804 (2006).
8. Kim, C., Park, J. & Blick, R. H. Spontaneous symmetry breaking in two coupled nanomechanical electron shuttles. *Phys. Rev. Lett.* **105**, 067204 (2010).
9. Bergeret, F. S., Virtanen, P., Heikkilä, T. T. & Cuevas, J. C. Theory of microwave-assisted supercurrent in quantum point contacts. *Phys. Rev. Lett.* **105**, 117001 (2010).
10. Talyanskii, V. I. et al. Single-electron transport in a one-dimensional channel by high-frequency surface acoustic waves. *Phys. Rev. B* **56**, 15180–15184 (1997).
11. Stadler, P., Belzig, W. & Rastelli, G. Ground-state cooling of a carbon nanomechanical resonator by spin-polarized current. *Phys. Rev. Lett.* **113**, 047201 (2014).
12. Urgell, C. et al. Cooling and self-oscillation in a nanotube electromechanical resonator. *Nat. Phys.* **16**, 32–37 (2020).
13. Gorelik, L. Y. et al. Shuttle mechanism for charge transfer in coulomb blockade nanostructures. *Phys. Rev. Lett.* **80**, 4526 (1998).
14. Gorelik, L. Y., Isacsson, A., Galperin, Y. M., Shekhter, R. I. & Jonson, M. Coherent transfer of Cooper pairs by a movable grain. *Nature* **411**, 454–457 (2001).
15. Isacsson, A., Gorelik, L. Y., Shekhter, R. I., Galperin, Y. M. & Jonson, M. Mechanical cooper pair transportation as a source of long-distance superconducting phase coherence. *Phys. Rev. Lett.* **89**, 277002 (2002).
16. Padurariu, C., Keijzers, C. J. H. & Nazarov, Yu. V. Effect of mechanical resonance on Josephson dynamics. *Phys. Rev. B* **86**, 155448(1)-155448(18) (2012).
17. Schneider, B. H., Etaki, S., van der Zant, H. S. J. & Steele, G. A. Coupling carbon nanotube mechanics to a superconducting circuit. *Sci. Rep.* **2**, 599(1)-599(5) (2012).
18. Hann, C. T. et al. Hardware-efficient quantum random access memory with hybrid quantum acoustic systems. *Phys. Rev. Lett.* **123**, 250501 (2019).
19. Chu, Y. et al. Creation and control of multi-phonon Fock states in a bulk acoustic-wave resonator. *Nature* **563**, 666–670 (2018).
20. Arrangoiz-Arriola, P. et al. Resolving the energy levels of a nanomechanical oscillator. *Nature* **571**, 537–540 (2019).
21. Bienfait, A. et al. Phonon-mediated quantum state transfer and remote qubit entanglement. *Science* **364**, 368–371 (2019).
22. Satzinger, K. J. et al. Quantum control of surface acoustic-wave phonons. *Nature* **563**, 661–665 (2018).
23. Girvin, S. M. Schrödinger cat states in circuit QED, arXiv:1710.03179v1 [quant-ph] (2017).
24. Hacker, B. et al. Deterministic creation of entangled atom-light Schrödinger-cat states. *Nat. Photonics* **13**, 110–115 (2019).
25. Houck, A. A., Koch, J., Devoret, M. H., Girvin, S. M. & Schoelkopf, R. J. Life after charge noise: recent results with transmon qubits. *Quantum Inf. Process* **8**, 105–115 (2009).
26. Kalashnikov, K. et al. Bifluxon: fluxon-parity-protected superconducting qubit. *PRX QUANTUM* **1**, 010307(1)-010307(15) (2020).
27. Peng, H. B., Chang, C. W., Aloni, S., Yuzvinsky, T. D. & Zettl, A. Ultrahigh frequency nanotube resonators. *Phys. Rev. Lett.* **97**, 087203 (2006).
28. Laird, E. A., Pei, F., Tang, W., Steele, G. A. & Kouwenhoven, L. P. A high quality factor carbon nanotube mechanical resonator at 39 GHz. *Nano Lett.* **12**, 193–197 (2012).
29. De Franceschi, S., Kouwenhoven, L., Schönenberger, C. & Wernsdorfer, W. Hybrid superconductor-quantum dot devices. *Nat. Nanotech.* **5**, 703–711 (2010).
30. Ming, X., Huang, H., Zorman, C. A., Mehregany, M. & Roukes, M. L. Nanodevice motion at microwave frequencies. *Nature* **421**, 496 (2003).
31. Armour, A. D., Blencowe, M. P. & Schwab, K. C. Entanglement and decoherence of a micromechanical resonator via coupling to a Cooper-pair box. *Phys. Rev. Lett.* **88**, 148301 (2002).
32. Voje, A., Kinaret, J. M. & Isacsson, A. Generating macroscopic superposition states in nanomechanical graphene resonators. *Phys. Rev. B* **85**, 205415(1)-205415(5) (2012).
33. Xiong, B. et al. Generation of entangled Schrödinger cat state of two macroscopic mirrors. *Opt. Express* **27**, 13547–13558 (2019).
34. Hou, Q., Yang, W., Chen, C. & Yin, Z. Generation of macroscopic Schrödinger cat state in diamond mechanical resonator. *Sci. Rep.* **6**, 37542 (2016).

ACKNOWLEDGEMENTS

This work was supported by the Croatian Science Foundation, project IP-2016-06-2289, by the QuantiXLie Centre of Excellence, a project co-financed by the Croatian Government and European Union through the European Regional Development Fund—the Competitiveness and Cohesion Operational Programme (Grant KK.01.1.1.01.0004), and by IBS-R024-D1. H.C.P. acknowledges the support from KIAS. J.S. acknowledges the support from KRISS (GP2021-0010-04) and NRF (2016R1A5A1008184). The authors thank Chulki Kim (KIST) for the fruitful discussion about the experimental feasibility of our findings.

AUTHOR CONTRIBUTIONS

D.R., L.Y.G., and S.-J.C. performed the analytic and numerical calculations. H.C.P., R.I.S., and L.Y.G. organized the project and J.S. estimated and discussed experimental perspectives. All authors analyzed the results, discussed, and wrote the paper. D.R. and S.-J.C. contributed equally to this work.

COMPETING INTERESTS

The authors declare no competing interests.

ADDITIONAL INFORMATION

Supplementary information The online version contains supplementary material available at https://doi.org/10.1038/s41534-022-00584-6.

Correspondence and requests for materials should be addressed to Hee Chul Park.

Reprints and permission information is available at http://www.nature.com/reprints

Publisher's note Springer Nature remains neutral with regard to jurisdictional claims in published maps and institutional affiliations.